processes

MDPI

Article

Prediction of the Effect of Fly Ash on the Unconfined Compressive Strength of Basalt Fiber Reinforced Clay Using Artificial Neural Networks

Yasemin Aslan Topçuoğlu

Department of Geological Engineering, Firat University, Elazığ 23119, Türkiye; yaslan@firat.edu.tr

Abstract: In this study, the effects of fly ash (FA) and basalt fiber (BF) additives on the unconfined compressive strength (q_u) of kaolin clay were experimentally investigated, and a dataset was created based on the results. This dataset was used in an artificial neural network (ANN) model to predict the q_u based on the additive ratio, water content, and curing time. For this purpose, samples were prepared by adding 1% BF with a length of 24 mm and FA at ratios of 3%, 6%, 9%, 12%, and 15% to the clay, followed by the addition of 25% and 30% water. Unconfined compressive tests were performed before curing and after 28, 42, and 56 days of curing to determine the q_u values. The evaluation of the obtained experimental results was carried out by creating an ANN model. To validate the prediction capabilities of the ANN, a comparative analysis was performed using various artificial intelligence models, and the model's overall performance was assessed with a 5-fold cross-validation technique. The evaluations revealed that the ANN model, using data from experimental studies, demonstrated the highest prediction accuracy and was in close agreement with the experimental results. According to the results obtained, the R value of the ANN model was calculated as 0.97, while the RMSE values were found as 0.09, 0.10, 0.06 and 0.04 for pre-curing, 28th day, 42nd day and 56th day, respectively.

Keywords: artificial neural network; basalt fiber; chemical stabilization; fly ash; kaolin; reinforcement; strength

check for updates

Academic Editors: Honggang Chen, Yuan Li and Junyu Guo

Received: 30 November 2024
Revised: 31 December 2024
Accepted: 6 January 2025
Published: 8 January 2025

Citation: Aslan Topçuoğlu, Y. Prediction of the Effect of Fly Ash on the Unconfined Compressive Strength of Basalt Fiber Reinforced Clay Using Artificial Neural Networks. *Processes* **2025**, *13*, 157. https://doi.org/10.3390/pr13010157

Copyright: © 2025 by the author. Licensee MDPI, Basel, Switzerland. This article is an open access article distributed under the terms and conditions of the Creative Commons Attribution (CC BY) license (https://creativecommons.org/licenses/by/4.0/).

1. Introduction

Soils in the field where engineering projects may be carried out may not always have engineering properties suitable for the project, i.e., they may have low strength and bearing capacity, high compressibility or high hydraulic permeability. In such cases, it is possible to make changes in the project design in order to eliminate the problem. However, soil stabilization methods are generally used. One of these methods emerges from recent studies involving the use of fibers. In these studies, soils can be reinforced by adding fibers, such as carbon, glass, polypropylene, and basalt fibers [1–9]. One of these types of fiber, basalt fiber (BF), is derived from volcanic rock and has a wide distribution in nature. BF is important due to its high strength, environmental friendliness, and the fact that its raw material is natural and abundant. The use of BF in soil reinforcement has increased in recent years, and it has been demonstrated in various studies that fiber reinforcement improves soil properties [1,10–14].

Another method is the chemical stabilization method. With this method, additives with pozzolanic properties are added to the soil, resulting in improvement in soil properties as a result of the pozzolanic reaction between the soil and the additives. In order to improve

clayey soils, some materials, such as lime, cement, silica fume, fly ash (FA), volcanic tuff and volcanic glass, are added into clays. The changes in the engineering properties of the soil samples with additives are examined, and the most suitable additive ratio and curing time are attempted to be determined. In the studies conducted, it has been reported that soil properties improve with the use of additives [15–18]. In the study by Vukicevic et al. [19], an investigation was conducted on alternative waste materials (FA and slag), which can be used in soil. The experimental results demonstrated that clay stabilization using FA has positive effects in terms of increasing strength and stiffness while reducing expansivity. In the study conducted by Abdila et al. [20], ground granulated blast slag (GGBS) and FA-based geopolymer processes were utilized for soil stabilization. The study noted that the presence of GGBS and FA particles filled the voids between clay soil particles, contributing to the formation of a stable and compact clay soil structure, thereby enhancing compression strength. Abdila et al. [21] investigated the use of FA and ground granulated blast furnace slag (GGBFS)-based geopolymers for soil stabilization. The researchers suggested that GGBFS and FA-based geopolymers could successfully be used as binders. It was noted that the use of stabilizing materials resulted in a significant increase in the q_u of clay soils. In the study by Turan et al. [22], the effects of class C and F FA on the mechanical and microstructural behavior and stabilization of clay soils were examined. According to the results of the experimental investigations, the addition of FA and increase in curing time improved the strength parameters and permeability of the stabilized soil. while reducing compression and swelling indices. In the study conducted by Mustafayeva et al. [23], the use of basic oxygen furnace (BOF) slag, a byproduct of steel production, was investigated for the strengthening of kaolin clay. The experimental results showed that higher BOF content and extended curing times improved soil strength, while lime and ground granulated blast-furnace slag effectively enhanced stabilization properties. In a limited number of studies, it has been noted that the use of various additives along with fibers leads to significant improvements in soil strength [24–27].

In studies involving the use of fibers and various additives, different additive ratios, water contents, and fiber lengths are utilized to identify changes in soil properties and achieve optimal values. A similar approach is adopted in studies aimed at determining the unconfined compressive strength (q_u) of soils, where these parameters are often selected randomly. However, intelligent systems can be used to help reduce time, cost, and labor in determining the optimal additive material, water content, and curing period that yield the highest q_u.

Methods such as artificial neural networks (ANNs), genetic algorithms, fuzzy logic, and particle swarm optimization are used to assess the strength of soils reinforced with various types of additives. Some of the studies are as follows.

In studies where various additives were used to improve soil properties, that by Tabarsa et al. [28] compared two artificial intelligence-based models, including ANN and support vector machines, to predict the strength properties of soils treated with cement, lime, and rice husk ash under different conditions. It was reported that the proposed models accurately predicted the q_u of the soils and could be presented as reliable prediction models in geotechnical engineering. In the study conducted by Aljanabi and Salih [29], a mixture composed of iron ore, used motor oil, shale rock powder, hydrated lime, gypsum, and cement was used in soil, along with various additives such as waste plastic pieces, rice husk, and sandstone powder. The study concluded that the proposed ANN model showed good accuracy in predicting the q_u of clay soils. In the study by Chumacero et al. [30], the effect of natural hydraulic lime, plastic, and metallic fiber additives on the geological properties of a gravelly clay soil was evaluated using an artificial intelligence model. The model suggests reducing dominant materials, such as lime, to obtain acceptable results

based on real test data. In the study by Krishna et al. [31], various additives, such as FA, lime, and cement, were added to the soil, and an ANN-based model was developed to predict the California Bearing Ratio (CBR) and Unconfined Compressive Strength (UCS). The results obtained generally indicate that ANN is an effective and reliable technique for predicting CBR and UCS.

In the study by Garg et al. [32], different fibers, such as polypropylene, water hyacinth, jute, and coconut, were used as reinforcements in soil. Models were developed using Extreme Learning Machine (ELM) to calculate the compressive strength of the reinforced soil. It was reported that the prediction accuracy of the ELM models in estimating the compressive strength of fiber-reinforced soil was reasonable. In the study by Tiwari and Satyam [33], the effects of pond ash and polypropylene fiber on soil strength were examined and it was reported that the results of the developed ANN model accurately predicted the mechanical properties. Ndepete et al. [34] characterized the behavior of BF-reinforced silty soil at different ratios (1%, 1.5%, and 2%) and various lengths (6, 12, and 24 mm) using machine learning models. It was reported that fiber length and cell pressure have a significant impact on the predictions of maximum deviator stress. In the study conducted by Sungur et al. [35], the shear strength of samples reinforced with different ratios of glass fiber (0%, 1%, 1.5%, and 2%) and at various water contents (13%, 15%, and 17%) was predicted using the ANFIS (Adaptive Neuro-Fuzzy Inference System). It was determined that the ANFIS model provided the best results for predicting shear strength when 80% of the data were used for training and 20% for testing. Sert et al. [36] prepared mixtures for experiments by using BF at 1%, 2%, and 3% ratios with different water contents and fiber lengths in a highly plastic clay. In the study, the highest strength was determined as approximately 880 kPa by mixing 24 mm fibers at 1% and 2% ratios with 15% water content. Additionally, the obtained dataset was used to train machine learning algorithms. The researchers stated that the decision tree regression showed superior performance in predicting stress and strain. Although there are studies on this subject using various fibers, these remain limited.

In this study, FA and BF additives were utilized to improve the strength properties of kaolin clay. FA, which is generated in large quantities as a byproduct from thermal power plants, poses environmental challenges due to disposal issues, contributing to pollution. Investigating the use of FA in various applications is crucial for reducing environmental impacts. In recent years, various fibers have been employed to enhance soil properties, with BF emerging as a particularly noteworthy material due to its natural origin from basalt, abundance, eco-friendliness, and, most importantly, its high strength properties. While there have been separate studies on the use of FA and BF as soil additives, research on their combined use remains limited. Therefore, exploring the combined effects of FA and BF on the q_u of soils is of significant importance. To address this gap in the literature, this study selects FA and BF as the additives of interest. Furthermore, artificial intelligence (AI) methods, which have become increasingly popular in various applications in recent years, are now widely employed in geotechnical engineering. Although studies on the application of AI methods in soil improvement are available, there is no research examining the impact of FA and BF additives on the q_u of clay soils using AI methods. This study aims to contribute to the evaluation of FA as an environmentally hazardous industrial byproduct and to promote more cost-effective soil stabilization practices through the combined use of FA and BF. Moreover, it is anticipated that this research will help fill existing gaps in applying AI methods in the field of geotechnical engineering. For this reason, the variation in q_u values in clay soils, with the addition of BF and FA, was analyzed based on curing time, and the mixture ratios and curing time providing maximum strength improvement were evaluated using the ANN method. The purpose of these evaluations is to predict

the additive material ratio, water content, and curing time that would achieve maximum q_u using ANN, eliminating the need for extensive experimental work. ANN allows for the quick prediction of optimum mixture ratios that yield maximum improvement in q_u at various curing times without conducting numerous experiments. Therefore, the use of ANN provides several advantages, such as savings in materials, labor, time, and cost reduction. Particularly, the time required to determine the optimum curing period, which may take days or months, can be significantly reduced, impacting both time and cost in studies in the fields of geology and civil engineering. Consequently, ANN is preferred in a wide range of fields, including geological engineering, civil engineering, and materials engineering [37–40]. Thus, using models created with the dataset defined in this study offers researchers a more practical tool for assessing q_u values.

The research questions of this study are presented below.

1. How do the combined effects of BF and FA additives influence the q_u of kaolin clay, and how can these effects be evaluated under varying water content, additive ratios, and curing durations?

2. How accurately can the effects of BF and FA additives on the unconfined compressive strength of kaolin clay be predicted using ANN-based models?

Experimental studies have been conducted, and ANN-based models have been developed to address the research questions. This paper is structured as follows: Section 2 provides details on the materials used, experimental methods, the experimental studies conducted, and the ANN approach. Section 3 presents the evaluation of the experimental results and compares the outcomes obtained from the experiments with the predictions made using the ANN technique. The model's accuracy is assessed based on R and RMSE values. Section 4 discusses all the experimental findings and explains the real-world applications of BF and FA in soil reinforcement.

2. Materials and Methods

2.1. Experimental Analysis

In this study, kaolin clay was used as the soil to be reinforced and BF and FA were used as additives. The clay was obtained from the Balıkesir-Sındırgı (Türkiye) clay quarry (Figure 1a). The liquid limit of kaolin clay is 45%, the plastic limit is 24%, and the plasticity index is 21%. According to the Unified Soil Classification System (USCS), this is classified as low-plasticity clay (CL) [13]. The optimum water content (w_{opt}) value of kaolin clay was determined to be 25.00%, and the maximum dry density (γ_{kmax}) value was determined to be 13.01 kN/m^3 [14]. The chemical analysis results of clay used in the study were obtained from the company where the clay was purchased, and its chemical properties are given in Table 1.

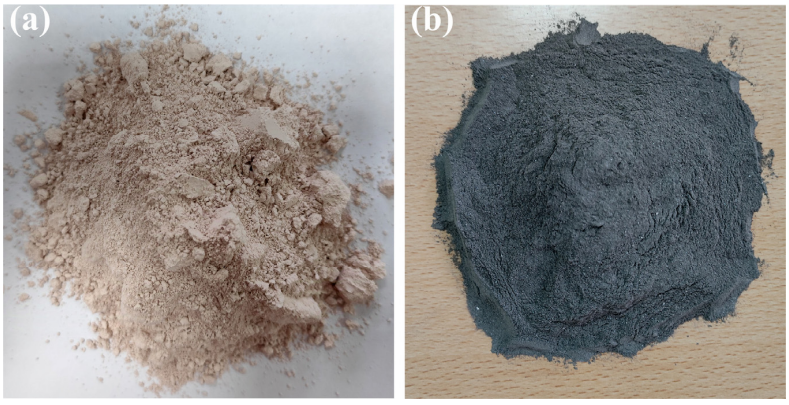


Figure 1. Kaolin clay (**a**) and FA (**b**) used in the study.

Table 1. Chemical analysis results of K and FA.

Main Oxides (%)	K	FA
SiO_2	69.00	29.20
Al_2O_3	12–17	11.30
Fe_2O_3	0.50	6.18
MgO	-	2.84
CaO	0.10	34.20
Na_2O	0.20	2.01
K_2O	≤13.17	0.71
MnO	-	0.05
TiO_2	<0.01	0.63
P_2O_5	-	0.42
SO_3	≤7.05	9.78
Sr	-	0.05
Cr_2O_3	0.01	0.04
Loss on ignition	-	3.60

The FA used in this study is from the lignite coal used as fuel in the Afşin-Elbistan (Kahramanmaraş, Türkiye) Thermal Power Plant (Figure 1b) and the chemical composition of the FA [41] is as in Table 1.

BF is obtained from a natural material called basalt, which is a dark-colored, fine-grained volcanic rock. When examined chemically, the major component forming the basalt is SiO_2 and the second major component is Al_2O_3. These two major components are followed by Fe_2O_3, FeO, CaO and MgO [42]. The BF used in this study is 24 mm in length (Figure 2a). The mechanical and physical properties of the BF were obtained from the company where the fiber was purchased (Spinteks Textile Construction Industry and Trade Inc.,Denizli, Türkiye). The mechanical and physical properties of the BF used in this study are as follows: fiber length: 24 mm, monofilament diameter: 15 ± 1.5 μm, maximum humidity: 2%, modulus of elasticity: 90 GPa, tensile strength: 3000 MPa, thermal conductivity: 0.031–0.038 W/mK, elongation at break: 3.5%, and density: 2.63 g/cm^3.

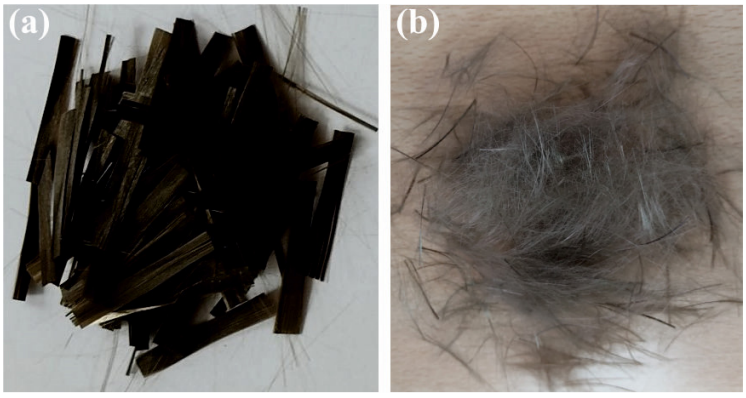


Figure 2. Unseparated (**a**) and separated (**b**) BF used in the study.

The experimental studies carried out within the scope of this study consist of unconfined compression tests performed before and after curing on unreinforced and reinforced kaolin clay. All experimental studies were carried out in the Rock-Soil Mechanics Laboratory of the Department of Geological Engineering of the Firat University, Elazığ, Türkiye.

Samples containing additives at BF (1) and FA (3, 6, 9, 12, and 15%) ratios were prepared during the preparation phase of the untreated and treated samples to be used in the experimental studies (Table 2). In the study conducted by [13], the optimum BF ratio at which the q_u value is maximum was determined to be 1%, and therefore, in this study,

the BF reinforcement ratio was also chosen as 1%. Mixtures were prepared using both the optimum water content of 25% for unreinforced kaolin clay and 30% water content to control the decrease in water content when FA was added. After the BF and FA ratios were decided, the preparation of mixtures and the compression of samples were carried out. First, the separation process was carried out in BF using a compressor (Figure 2b). After K and FA were dried in an oven at 105 °C for 24 h, a predetermined amount of K and FA separated BF was added and thoroughly mixed with the help of a mixer (Figure 3a). In this study, both the mixer and manual mixing methods were applied, and the duration of the mixing process was chosen as 10 min to ensure a complete and homogeneous mixture. Distilled water at ratios of 25% and 30% was evenly sprayed onto the prepared mixtures and mixed again with a mixer. Then, the prepared mixtures were compacted using Standard Proctor tests according to ASTM D698-12e2 [43] standard (Figure 3b). Samples with dimensions that can be used in the unconfined compression test were taken from the samples compressed in the mold with water contents of 25% and 30% (Figure 3c).

Table 2. Water, BF and FA ratios of the mixtures used in unconfined compression test.

Water Content (%)	Sample Number	K (%)	BF (%)	FA (%)
25	K	100	0	0
	K + 1%BF	99	1	0
	K + 1%BF + 3%FA	96	1	3
	K + 1%BF + 6%FA	93	1	6
	K + 1%BF + 9%FA	90	1	9
	K + 1%BF + 12%FA	87	1	12
	K + 1%BF + 15%FA	84	1	15
30	K	100	0	0
	K + 1%BF	99	1	0
	K + 1%BF + 3%FA	96	1	3
	K + 1%BF + 6%FA	93	1	6
	K + 1%BF + 9%FA	90	1	9
	K + 1%BF + 12%FA	87	1	12
	K + 1%BF + 15%FA	84	1	15

K: Kaolin Clay, BF: Basalt fiber; FA: Fly Ash.

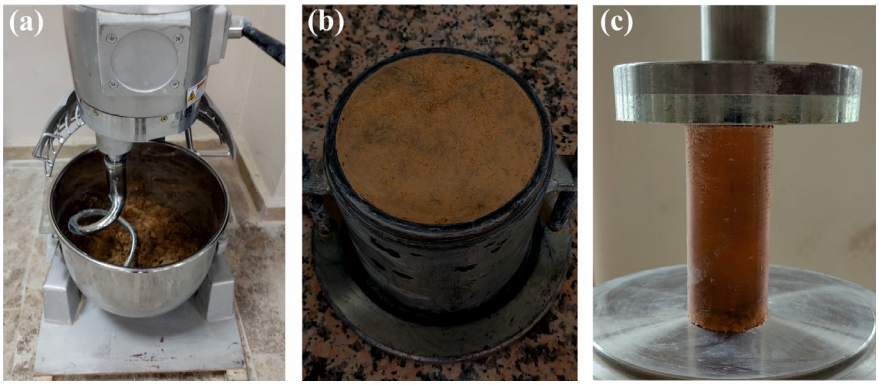


Figure 3. Mixing of K, FA and BF mixtures in the mixer (**a**), compressed sample (**b**), samples taken for the unconfined compression test (**c**).

The unconfined compression tests were performed in 45 samples before curing, and in 130 samples after 28, 42 and 56 days of curing, according to ASTM D2166M-16 [44] standard (Figure 4). Thus, q_u values of the samples were determined before and after curing. To determine the q_u values of the samples, cylindrical soil specimens with a height of 76 mm

and a diameter of 38 mm were extracted from mixtures compacted in a standard Proctor mold and subjected to unconfined compression tests. The average q_u values of the mixtures are given in Table 3.

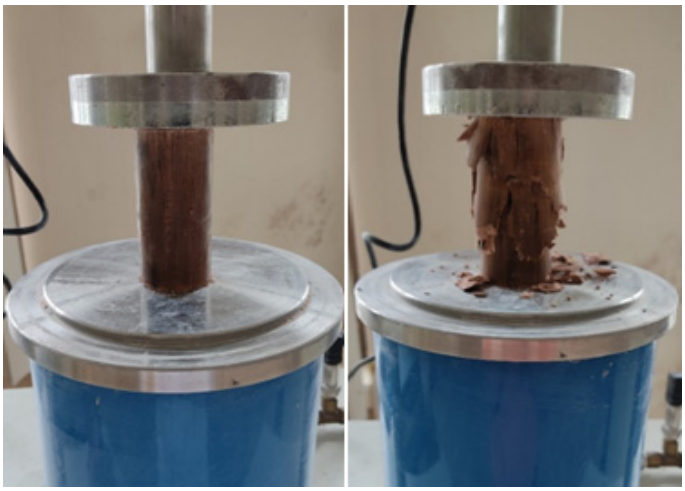


Figure 4. Examples before and after the unconfined compression test.

Table 3. Unconfined compression test results of K + BF + FA mixtures.

Sample Number	Water Content (%)	Pre-Curing (kPa) (Average)	Post-Curing (kPa) (Average)		
			28-Day	42-Day	56-Day
K	25	285.65	288.77	290.82	291.25
K + 1%BF		790.25	792.89	793.67	796.33
K + 1%BF + 3%FA		538.16	592.75	638.35	666.39
K + 1%BF + 6%FA		622.01	762.09	855.01	909.19
K + 1%BF + 9%FA		712.81	820.19	1061.36	1103.04
K + 1%BF + 12%FA		649.80	723.76	791.75	830.16
K + 1%BF + 15%FA		510.70	609.01	653.72	699.81
K	30	87.51	89.33	90.19	91.47
K + 1%BF		591.70	594.33	595.43	598.67
K + 1%BF + 3%FA		697.93	864.24	1052.37	1072.40
K + 1%BF + 6%FA		742.96	989.77	1307.60	1354.84
K + 1%BF + 9%FA		849.94	1092.74	1593.47	1641.61
K + 1%BF + 12%FA		739.69	912.30	1018.38	1059.16
K + 1%BF + 15%FA		663.12	774.51	868.90	912.62

2.2. Artificial Neural Network

In this study, the q_u values of samples prepared using FA and BF as additives were measured experimentally, and the q_u was estimated by artificial intelligence. The goal of this model is to predict q_u values based on varying ratios of BF, FA, clay, and water offering a data-driven method for assessing material strength and eliminating the need for additional physical testing.

In the study, an ANN technique, which is one of the artificial intelligence techniques and works like a biological neural network, was used [45,46]. ANNs consist of layers of interconnected nodes (or neurons), where each node represents a mathematical function. These networks learn relationships from data through a process called training, which involves adjusting the weights of connections between nodes in order to minimize the error in predictions or classifications. The architecture of an ANN can vary in complexity, ranging from simple single-layer perceptrons to deep neural networks with multiple layers.

The ANN was chosen for its ability to efficiently process complex, nonlinear data, making it particularly suitable for estimating q_u in mixtures with diverse reinforcement proportions [45,47]. Additionally, ANN's rapid prediction capability provides a valuable tool for applications requiring prompt decision-making—such as civil engineering, materials engineering, and geotechnical engineering—where time savings directly impact project schedules and costs [37–40].

To develop the ANN, an extensive experimental dataset was collected, from which q_u values were systematically derived and subsequently used to train the network. The structure of the ANN model in this study consists of input, hidden, and output layers as seen in Figure 5. The model takes key variables as inputs—namely, the clay content ratio, BF ratio, FA ratio and water content—and processes them through a hidden layer. In more intricate models, multiple hidden layers may enhance learning capacity, but this can also increase computational complexity and processing times. For this study, a single hidden layer was determined to be optimal, striking a balance between computational efficiency and prediction accuracy based on the dataset characteristics.

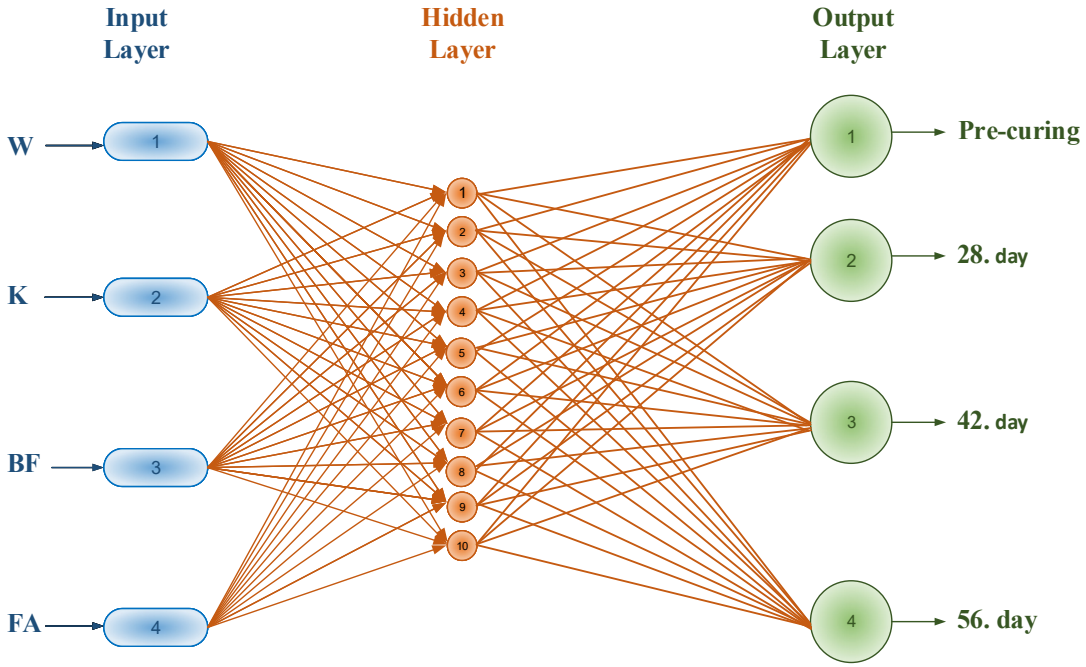


Figure 5. The ANN structure.

Data samples were divided into subsets for training, testing, and validation. During training, the ANN learned to generate q_u predictions for given inputs under specified conditions, thereby refining its ability to produce accurate outcomes. Following training, experimental data were organized in lookup tables and input into the ANN system to facilitate straightforward q_u prediction. Consequently, the ANN's output provides a reliable estimate of q_u, streamlining the assessment process and delivering consistent predictions that enhance both efficiency and reliability in material performance evaluations.

Overall, the ANN approach offers a highly effective, cost-efficient solution for modeling q_u in BF/FA-reinforced clay, providing a practical and adaptable tool for geotechnical applications.

3. Results

3.1. Experimental Results

According to the experimental results, it was determined that the q_u values increased in samples prepared with both 25% and 30% water content when 1% BF was added to

the unreinforced clay. It can be said that BF reinforcement significantly increased the q_u value of the clay. In samples prepared with 25% water content, the maximum q_u value before curing was determined to be 712.81 kPa in the K + 1%BF + 9%FA sample. In samples prepared with 30% water content, the maximum q_u value before curing was found to be 849.94 kPa, again in the K + 1%BF + 9%FA sample. When q_u values of the samples in which the BF contribution is fixed at 1% and the FA ratio is 3, 6 and 9% are examined, the q_u values of the samples with the water content of 25 and 30% increase with the increase of the FA additive, reaching the maximum value at the rate of 9% FA. On the other hand, it decreases in samples where FA ratio is 12 and 15%. When the post-curing q_u values are compared with the pre-curing q_u values of the untreated and BF additive treated samples, the changes are very limited. According to these results, it can be said that the curing application and the applied curing time do not have a significant effect on the strength of the untreated and 1% BF additive treated samples (Table 3).

With the effect of 28 days of curing, the q_u values of all BF and FA added samples increased significantly and the q_u values of these mixtures ranged from 592.75 to 1092.74 kPa. The example that gives the maximum strength is K + 1%BF + 9%FA, which has a 30% water content, and a significant increase in strength has occurred with the effect of curing compared to the untreated clay. After 42 days of curing, the strength values increased with increasing curing time. In the BF and FA additive treated samples, the maximum strength was determined 1593.47 kPa in the K + 1%BF + 9%FA sample prepared at 30% water content. After the application of the curing period as 56 days, the increase in the strength values of all BF and FA additive treated samples continued. The q_u values of these samples were between 598.67–1641.61 kPa, and the maximum strength value was determined in the 30% water added K + 1%BF + 9%FA sample. As a result, the maximum q_u value was determined in the K + 1%BF + 9%FA sample prepared with 30% water content after 56 days of curing. It was observed that the q_u values decreased in samples prepared with 12% and 15% FA added at both water contents during different curing times (Table 3).

3.2. Results of the ANN System

The ANN system developed for this study was created in Matlab R2022b. The results obtained with NN were also obtained in the Matlab environment.

In this study, a Single Layer Perceptron (SLP) neural network was employed. This type of network was selected due to its effectiveness in modeling simpler relationships between input and output variables.

The diagram of the ANN system used in this study incorporates four input variables, ten neurons within a single hidden layer, and four output variables, as shown in Figure 6. This network design was optimized for predicting the q_u based on input data collected from extensive experimental testing.

The Levenberg-Marquardt algorithm, known for its efficiency in training neural networks, was selected to improve the learning process of the model. This method combines the Gauss-Newton and gradient descent approaches, enabling rapid convergence when close to the best solution and stability when farther from it. The algorithm iteratively updates the model parameters, ensuring effective and stable convergence to the solution.

For model training and testing, a total of 42 data samples were utilized for each of the four input variables. To effectively train, validate, and test the model, 70% of these samples (30 data points) were allocated for training, while 15% (6 data points) were set aside for validation and the remaining 15% (6 data points) for testing.

Figure 7 provides a Simulink block diagram, which visualizes the ANN's output based on sample input values, demonstrating the system's architecture and function.

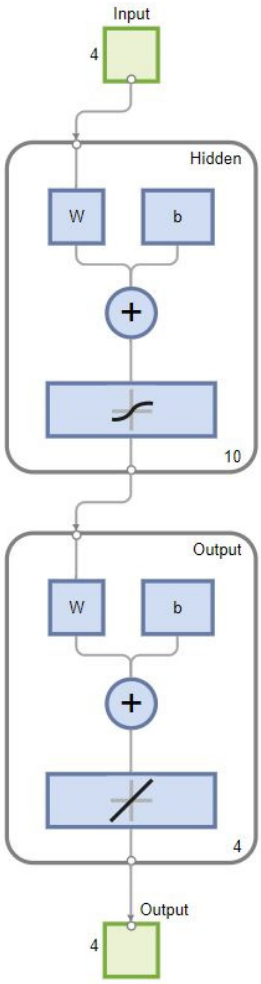


Figure 6. ANN diagram.

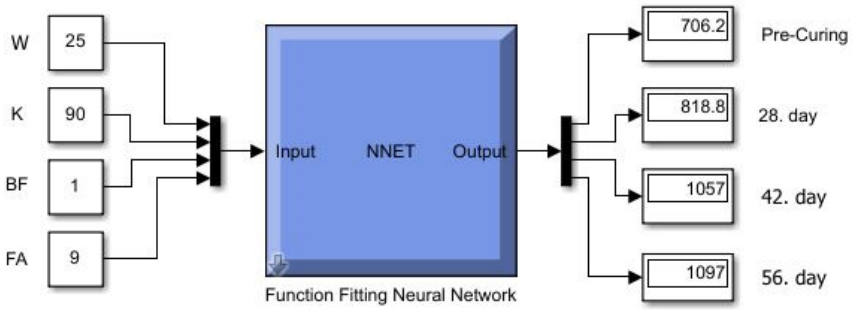


Figure 7. Sample results of ANN model.

A comprehensive review of Figure 7 and Table 3 together reveals a close match between the ANN predictions and experimental results, affirming the model's effectiveness in estimating q_u values accurately.

To measure the ANN model's predictive accuracy, root mean squared error (RMSE) was used as the performance metric, while regression (R) values were calculated to indicate the level of correlation between the ANN outputs and actual experimental results. RMSE is calculated by taking the square root of the average of the squared differences between the actual values and the predicted values. A lower RMSE indicates better model performance, as it shows less deviation between the predicted and actual values. R measures the strength of the linear relationship between the predicted and actual values. It is calculated by dividing the sum of the products of the deviations of the predicted and actual values

from their respective means by the product of the sum of the squared deviations of both sets. High R values, especially those approaching 1, signify strong agreement between the predicted and observed values, reflecting high model accuracy. Conversely, an R value close to 0 suggests a weak correlation, indicating lower model performance.

The *x*-axis labeled as 'target' in Figure 8 represents the actual output values derived from the dataset used in the training and validation of the ANN model. These target values serve as the ground truth against which the predicted values (represented on the *y*-axis) are compared. This comparison is essential for evaluating the performance of the ANN, through *R* metrics, which quantifies how well the predictions align with the actual data.

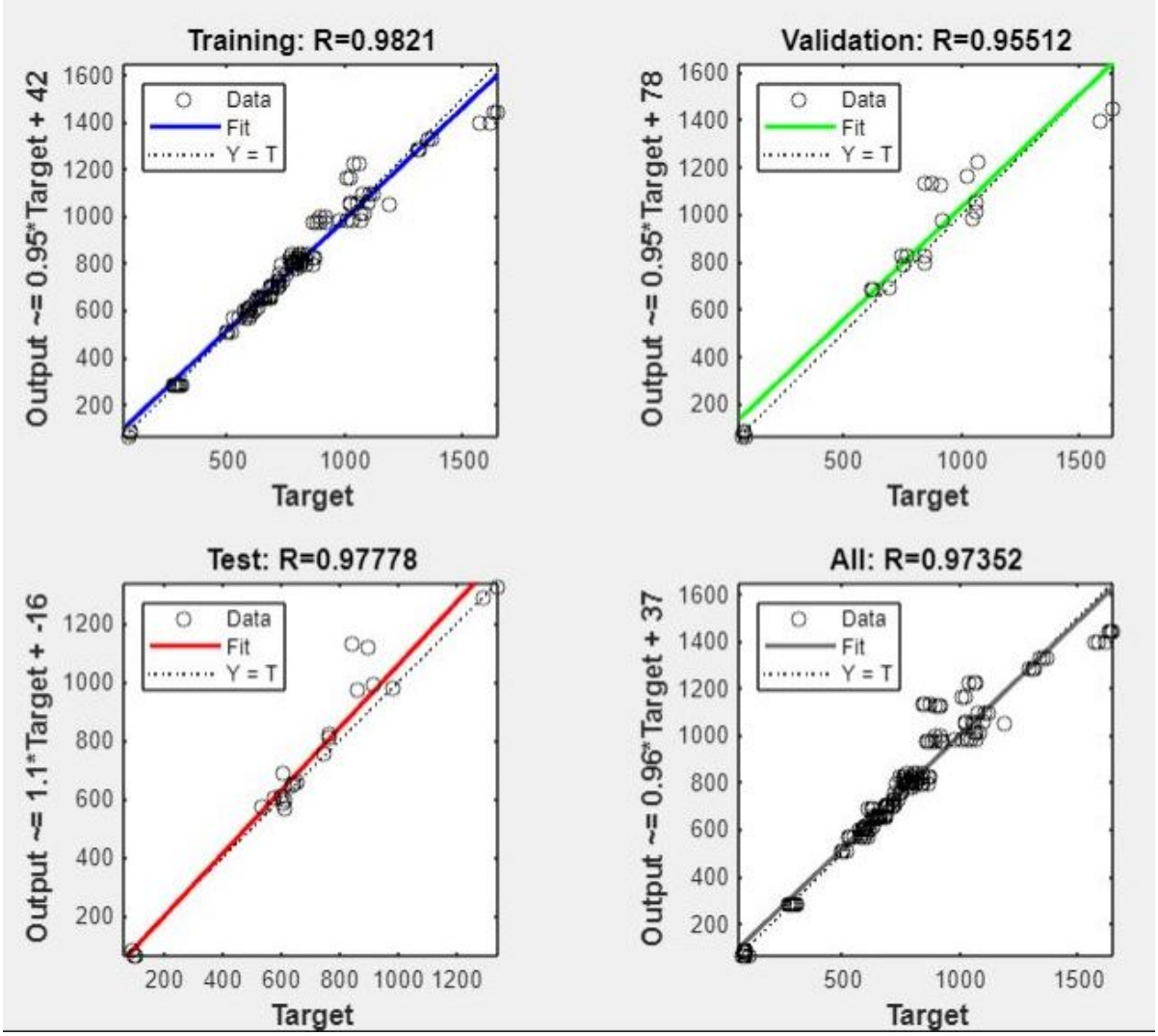


Figure 8. The R values of the ANN model.

As depicted in Figure 8, for this study, all R values were consistently close to 1, underscoring the ANN's strong predictive capability. The R value for total datasets were found to be 0.97.

After the ANN was trained, it was further evaluated with 14 test data. The R value obtained as a result of the test of the ANN model is 0.85 and the test regression graph is as given in Figure 9.

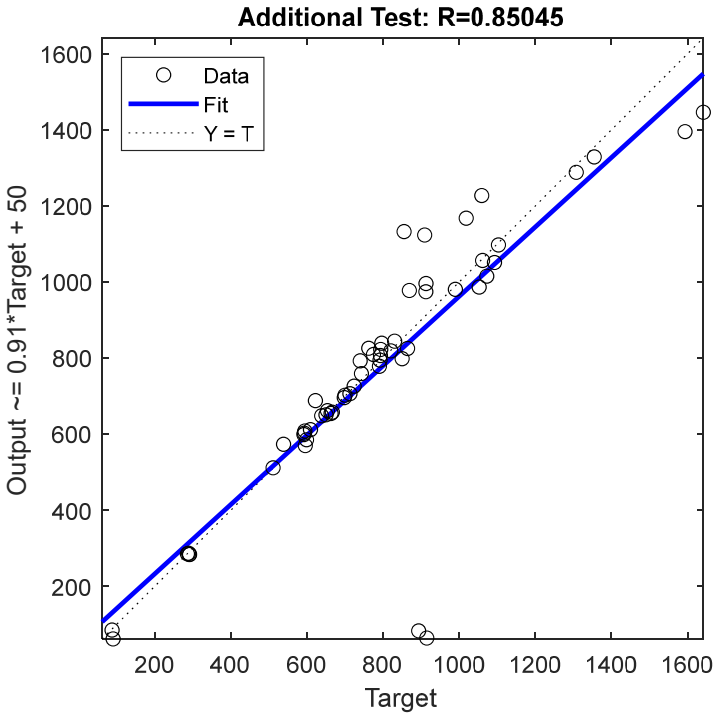


Figure 9. The test regression graph.

To assess the predictive accuracy of the ANN model, a comparative analysis was conducted against other artificial intelligence models, specifically Gaussian Process Regression (GPR), Support Vector Machines (SVM), Tree Regression (TR) and Linear Regression (LR).

While performing the comparison analysis, the cross-validation strategy detailed in the literature was applied to determine the reliability of the model [48,49]. This method minimizes the likelihood of creating a model overly dependent on a particular dataset and supports an objective assessment of the model's generalizability.

As presented in Table 4, the ANN model in both pre- and post-cure q_u values demonstrated the lowest RMSE value, underscoring its superior predictive performance relative to the other models. The closer the RMSE value is to zero, the less difference there is between the estimated data and the experimental data. In Table 4, it is seen that the difference between the estimate made using ANN and the actual results is very small.

Table 4. RMSE values for different AI models.

RMSE Value	NN	GPR	SVM	TR	LR
Pre-Curing	0.09	0.10	0.28	0.45	0.37
28 Day	0.10	0.11	0.26	0.58	0.35
42 Day	0.06	0.07	0.36	0.65	0.46
56 Day	0.04	0.05	0.30	0.63	0.39

Finally, a 5-fold cross-validation method was adopted to objectively evaluate the ANN model's in both pre-cure and post-cure (for 28, 42 and 56 day) q_u values performance and response plots of results based on the 5-fold cross-validation were presented in Figure 10a, 10b, 10c and 10d respectively. As seen in the figures, error rates between the system's predicted outputs (yellow) and actual values (blue) are very low.

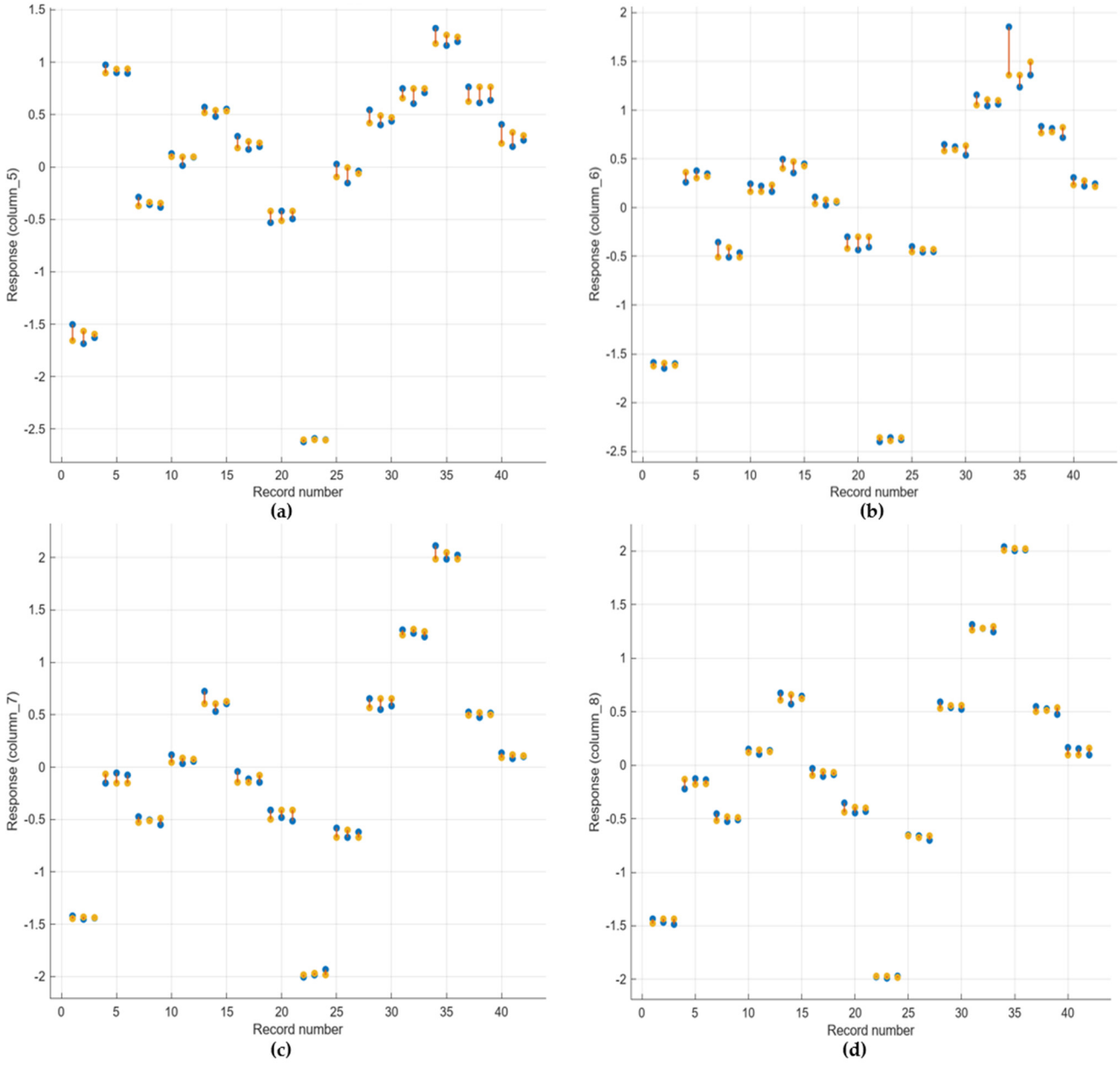


Figure 10. 5-fold-cross-validation response plot for (**a**) pre-curing (**b**) 28 day (**c**) 42 day (**d**) 56 day.

The figures were generated using the MATLAB environment, where the vertical axis represents the output values, and the horizontal axis denotes the number of data points. The yellow dots represent the predicted output values, while the blue dots correspond to the actual values. The red lines drawn between the yellow and blue dots illustrate the magnitude of the error between the predicted and actual values. Upon examining the red lines between the yellow and blue dots for each output value, it becomes evident that most error values are so small that they can only be discerned upon close inspection. This observation demonstrates the effectiveness of the ANN model, even when evaluated through 5-fold cross-validation.

4. Discussion

In this study, the use of BF and FA as additives in kaolin clay resulted in significant improvements in soil strength. It is clearly seen from the test results that the increase in the curing time and the FA ratio up to a certain optimum value is quite effective in increasing the strength. Similar studies involving the use of FA and various additives

have also reported increases in strength values [19–22]. In addition, experimental studies conducted by Turan et al. [22] and Mustafayeva et al. [23] also indicate that curing duration contributes to increasing strength values. The increase in strength values observed in this study, based on the addition of FA and curing duration, is consistent with other studies [19–22] in the literature. This increase in strength can be explained, in addition to the effect of BF, by the pozzolanic reactions that occur between clay and FA. With longer curing durations, the pozzolanic reactions between FA and clay progress, forming silicate gels that fill interparticle voids and bond the particles together, thereby enhancing strength [15,16,26,50–52].

The experimental results of the study indicate that, up to a certain ratio, the combined effects of BF and FA additives, along with water content, significantly enhance the q_u value of clay, with the curing period also playing a significant role in this improvement.

Additionally, the q_u values predicted by the ANN model developed using the dataset prepared from experimental studies showed significant agreement with the q_u values obtained from experimental results. This demonstrated the effectiveness of ANN in evaluating compressive strength performance. The fact that all R values for this study are consistently close to 1 indicates the strong predictive capability of the ANN. These findings from the experimental studies and ANN-based models fully validate the research questions.

The optimum fiber and FA content, water content, and curing duration values identified in this study can be utilized in experimental studies for low-plasticity kaolin clays; however, these ratios should be further investigated for different soil types. Therefore, conducting new studies by varying the BF content and length, FA ratio, water content, curing duration, and soil type will contribute to the development of a more comprehensive dataset on this subject. Furthermore, as the success of artificial intelligence models is associated with the number of input variables, future studies should focus on creating datasets with a larger number of experimental results to develop new ANN models.

Real-World Applications of BF and FA in Soil Reinforcement

Clay soils, characterized by high settlement potential and low bearing capacity, are often considered problematic in engineering applications. Therefore, mixtures of BF and FA can be regarded as an effective soil improvement method, particularly for enhancing the strength of surface clay soils in engineering practices. The findings of this study demonstrate that the addition of BF and FA significantly improves the strength of clay soils. As a result of this strength enhancement, clay soils stabilized with BF and FA can be used as a subbase layer in highway construction, helping to mitigate settlement issues. In building foundations, this stabilization method can increase the bearing capacity of the soil, providing a more reliable soil environment for foundation systems.

Additionally, problematic soils at greater depths can be improved using BF and FA mixtures. For instance, deep mixing techniques can effectively incorporate BF and FA into soil layers at desired depths to enhance their properties. This method can improve the strength of water-saturated clay soils, providing a more robust foundation for structures such as ports, docks, and similar facilities. Moreover, BF and FA mixtures can be used to enhance the safety of load-bearing soil layers during deep excavations for high-rise structures. Through applications reaching desired depths, deep mixing columns reinforced with BF and FA can be created, allowing structures to be built on a stronger and improved soil profile.

Furthermore, the utilization of FA, an industrial waste, in such applications contributes to environmental sustainability by preventing critical environmental impacts such as groundwater contamination. The combined use of BF and FA reduces the required amount of BF additive, resulting in a more cost-effective application.

5. Conclusions

In this study, unconfined compression tests were conducted both before and after curing on mixtures prepared with BF and FA additives in kaolin clay. According to the experimental results, the maximum q_u value was determined in the K + 1%BF + 9%FA sample prepared with 30% water content after 56 days of curing. Using the obtained data set, depending on the additive ratio and water content in the mixture, the pre- and post-cure q_u values was estimated with the ANN-based model. The estimation results made using ANN were compared with the experimental data and the R value of the model was calculated as 0.97. In addition, ANN, GPR, SVM, TR and LR techniques were compared using the 5-fold cross-validation method. Accordingly, ANN gave the most successful result in estimating the pre- and post-curing compressive strength. The RMSE values of the pre- and post-curing compressive strength estimated by ANN were obtained as 0.09, 0.10, 0.06 and 0.04 for pre-curing, 28th day, 42nd day and 56th day, respectively. The q_u values predicted by the ANN were in significant agreement with the experimental results, demonstrating the effectiveness of the ANN in evaluating compressive strength performance. The use of ANN offers advantages by saving time, materials, and labor for researchers. This study is important because it shows that the use of BF in soil reinforcement works will provide significant benefits due to its superior properties, such as being natural, sustainable, environmentally friendly, and having abundant raw material availability. In addition, the use of FA as an additive is of great importance in terms of preventing the environmental pollution and evaluating it economically because the amount produced in power plants is too high.

Funding: This research received no external funding.

Data Availability Statement: The original contributions presented in the study are included in the article, further inquiries can be directed to the corresponding author.

Conflicts of Interest: The author declares no conflicts of interest.

References

1. Gao, L.; Hu, G.; Xu, N.; Fu, J.; Xiang, C.; Yang, C. Experimental Study on Unconfined Compressive Strength of Basalt Fiber Reinforced Clay Soil. *Adv. Mater. Sci. Eng.* **2015**, *2015*, 561293. [CrossRef]
2. Lokre, P. Stabilization of Black Cotton Soil by Using Glass Fibres. *Int. J. Sci. Res. Dev.* **2020**, *8*, 573–578.
3. Bao, X.; Huang, Y.; Jin, Z.; Xiao, X.; Tang, W.; Cui, H.; Chen, X. Experimental Investigation on Mechanical Properties of Clay Soil Reinforced with Carbon Fiber. *Constr. Build. Mater.* **2021**, *280*, 122517. [CrossRef]
4. Kambale, N.; Rakkaraddi, P.G. Comparative Study of Soil Stabılization with Addition of Glass, Basalt and Polypropylene Fibres. *Int. J. Creat. Res. Thoughts (IJCRT)* **2022**, *10*, b674–b681.
5. Rabab'ah, S.; Al Hattamleh, O.; Aldeeky, H.; Abu Alfoul, B. Effect of Glass Fiber on The Properties of Expansive Soil and Its Utilization as Subgrade Reinforcement in Pavement Applications. *Case Stud. Constr. Mater.* **2021**, *14*, e00485. [CrossRef]
6. Sujatha, E.R.; Atchaya, P.; Darshan, S.; Subhashini, S. Mechanical Properties of Glass Fibre Reinforced Soil and Its Application as Subgrade Reinforcement. *Road Mater. Pavement Des.* **2021**, *22*, 2384–2395. [CrossRef]
7. Al-Kareem, K.W.A.; Fattah, M.Y.; Hameedi, M.K. Compressibility and Strength Development of Soft Soil by Polypropylene Fiber. *Int. J. Geomate* **2022**, *22*, 91–97. [CrossRef]
8. Hamza, M.; Ijaz, N.; Fang, C.; Ijaz, Z. Stabilization of Problematic Expansive Clays Using Polypropylene Fiber Reinforcement. *Jordan J. Civ. Eng.* **2022**, *16*, 531–539.
9. Rajabi, A.M.; Ghorashi, S.M.S.; Yeganeh, M.M. The Effect of Polypropylene and Glass Fibers on Strength and Failure Behavior of Clayey Sand Soil. *Arab. J. Geosci.* **2023**, *16*, 6. [CrossRef]
10. Ndepete, C.P.; Sert, S. Use of Basalt Fibers for Soil Improvement. *Acta Phys. Pol.* **2016**, *130*, 355–356. [CrossRef]
11. Kale, R.Y.; Dahake, N.D.; Sahu, S.M.; Gawande, G.A.; Wailker, P.J.; Patekar, V.R.; Pawar, C.R. Soil Stabilization by Using Basalt Fibers. *Int. J. Sci. Res. Eng. Trends* **2020**, *6*, 1931–1935.
12. Zhao, N.; Wu, H.; Huang, Z. Strength Behavior of Red Clay Reinforced by Basalt Chopped Fiber. *Arab. J. Geosci.* **2021**, *14*, 15. [CrossRef]

13. Gürocak, Z.; Topçuoğlu, Y.A. Bazalt Fiber Kullanımının Düşük Plastisiteli Kilin Serbest Basınç Dayanımı Üzerindeki Etkisi. *Gümüşhane Üniversitesi Bilim. Derg.* **2023**, *13*, 688–701. [CrossRef]
14. Topçuoğlu, Y.A.; Gürocak, Z. The Effect of Basalt Fiber Reinforcement at Different Ratios on The Unconfined Compressive Strength of Kaolin. *Niğde Ömer Halisdemir Üniversitesi Mühendislik Bilim. Derg.* **2024**, *13*, 169–175.
15. Rai, P.; Qiu, W.; Pei, H.; Chen, J.; Ai, X.; Liu, Y.; Ahmad, M. Effect of Fly Ash and Cement on The Engineering Characteristic of Stabilized Subgrade Soil: An Experimental Study. *Hindawi Geofluids* **2021**, *2021*, 1–11. [CrossRef]
16. Shirkhanloo, S.; Najafi, M.; Kaushal, V.; Rajabi, M. A Comparative Study on The Effect of Class C and Class F Fly Ashes on Geotechnical Properties of High-Plasticity Clay. *Civ. Eng.* **2021**, *2*, 1009–1018. [CrossRef]
17. Jassim, N.W.; Alsafi, S. Study The Consequence of Fly Ash on Some of Physical Soil Characteristics. *IOP Conf. Ser. Earth Environ. Sci.* **2022**, *961*, 012089. [CrossRef]
18. Randhawa, K.S.; Chauhan, R.; Kumar, R. An Investigation on the Effect of Lime Addition on UCS of Indian Black Cotton Soil. *Mater. Today Proc.* **2022**, *50*, 797–803. [CrossRef]
19. Vukićević, M.; Marjanović, M.; Pujević, V.; Jocković, S. The Alternatives to Traditional Materials for Subsoil Stabilization and Embankments. *Materials* **2019**, *12*, 3018. [CrossRef] [PubMed]
20. Abdila, S.R.; Abdullah, M.M.A.B.; Ahmad, R.; Rahim, S.Z.A.; Rychta, M.; Wnuk, I.; Nabiałek, M.; Muskalski, K.; Tahir, M.F.M.; Gucwa, M.; et al. Evaluation on the Mechanical Properties of Ground Granulated Blast Slag (GGBS) and Fly Ash Stabilized Soil Via Geopolymer Process. *Materials* **2021**, *14*, 2833. [CrossRef] [PubMed]
21. Abdila, S.R.; Abdullah, M.M.A.B.; Ahmad, R.; Burduhos Nergis, D.D.; Rahim, S.Z.A.; Omar, M.F.; Sandu, A.V.; Vizureanu, P.; Syafwandi. Potential of soil stabilization using ground granulated blast furnace slag (GGBFS) and fly ash via geopolymerization method: A review. *Materials* **2022**, *15*, 375. [CrossRef]
22. Turan, C.; Javadi, A.A.; Vinai, R. Effects of class C and class F fly ash on mechanical and microstructural behavior of clay soil—A comparative study. *Materials* **2022**, *15*, 1845. [CrossRef] [PubMed]
23. Mustafayeva, A.; Bimykova, A.; Olagunju, S.O.; Kim, J.; Satyanaga, A.; Moon, S.W. Mechanical Properties and Microscopic Mechanism of Basic Oxygen Furnace (BOF) Slag-Treated Clay Subgrades. *Buildings* **2023**, *13*, 2962. [CrossRef]
24. Özdemir, T.; Polat, G.E.; Azdeniz, O.; Boz, A.; Sezer, A. Strength Properties of Clay Soil Reinforced with Basalt Fiber and Lime. In Proceedings of the Zemin Mekaniği ve Geoteknik Mühendisliği 16. Ulusal Kongresi, Erzurum, Türkiye, 13–14 October 2016; pp. 1025–1034.
25. Boz, A.; Sezer, A.; Özdemir, T.; Hızal, G.E.; Azdeniz Dolmacı, O. Mechanical Properties of Lime-Treated Clay Reinforced with Different Types of Randomly Distributed Fibers. *Arab. J. Geosci.* **2018**, *11*, 1–14. [CrossRef]
26. Ma, Q.Y.; Cao, Z.M.; Yuan, P. Experimental Research on Microstructure and Physical-Mechanical Properties of Expansive Soil Stabilized with Fly Ash, Sand, And Basalt Fiber. *Adv. Mater. Sci. Eng.* **2018**, *2018*, 9125127. [CrossRef]
27. Sharo, A.A.; Alawneh, A.S.; Al Zghool, H.N.; Rabab'ah, S.R. Effect of Alkali-Resistant Glass Fibers and Cement on The Geotechnical Properties of Highly Expansive Soil. *J. Mater. Civ. Eng.* **2022**, *34*, 04021417. [CrossRef]
28. Tabarsa, A.; Latifi, N.; Osouli, A.; Bagheri, Y. Unconfined Compressive Strength Prediction of Soils Stabilized Using Artificial Neural Networks and Support Vector Machines. *Front. Struct. Civ. Eng.* **2021**, *15*, 520–536. [CrossRef]
29. Aljanabi, K.R.M.; Salih, N.B. Using Artificial Neural Networks to Predict the Unconfined Compressive Strength of Clayey Soils Stabilized by Various Stabilization Agents. *KSCE J. Civ. Eng.* **2023**, *27*, 3720–3728. [CrossRef]
30. Chumacero, J.M.G.; Torres, P.L.A.; La Portilla, C.C.C.; Perez, S.P.M. Influence of Artificial Intelligence on the Optimization of the Dosage of Natural Hydraulic Lime, Plastic and Metallic Fibers on the Geological Characteristics of a Treated Soil. *Rev. Ing. Construcción* **2023**, *38*, 473–484. [CrossRef]
31. Krishna, S.V.; Santosh, B.S.; Prasanth, B.S. Prediction of UCS and CBR of A Stabilized Black-Cotton Soil Using Artificial Intelligence Approach: ANN. *Mater. Today Proc.* **2023**. [CrossRef]
32. Garg, A.; Bordoloi, S.; Mondal, S.; Ni, J.J.; Sreedeep, S. Investigation of Mechanical Factor of Soil Reinforced with Four Types of Fibers: An Integrated Experimental and Extreme Learning Machine Approach. *J. Nat. Fibers* **2020**, *17*, 650–664. [CrossRef]
33. Tiwari, N.; Satyam, N. Coupling Effect of Pond Ash and Polypropylene Fiber on Strength and Durability of Expansive Soil Subgrades: An Integrated Experimental and Machine Learning Approach. *J. Rock Mech. Geotech. Eng.* **2021**, *13*, 1101–1112. [CrossRef]
34. Ndepete, C.P.; Sert, S.; Beycioğlu, A.; Katanalp, B.Y.; Eren, E.; Bağrıaçık, B.; Topolinski, S. Exploring the Effect of Basalt Fibers On Maximum Deviator Stress and Failure Deformation of Silty Soils Using ANN, SVM and FL Supported by Experimental Data. *Adv. Eng. Softw.* **2022**, *172*, 103211. [CrossRef]
35. Sungur, A.; Keskin, N. Prediction of The Shear Strength of Glass Fiber-Reinforced Clay Soil by Adaptive Neuro-Fuzzy Inference System (ANFIS). *El-Cezeri* **2022**, *9*, 1255–1264.
36. Sert, S.; Arslan, E.; Ocakbaşı, P.; Ekinci, E.; Garip, Z.; Özocak, A.; Bol, E.; Ndepete, C.P. Stabilization of Expansive Clays with Basalt Fibers and Prediction of Strength by Machine Learning. *Arab. J. Sci. Eng.* **2024**, *49*, 13651–13670. [CrossRef]

37. Demir, T.; Duranay, Z.B.; Demirel, B.; Yildirim, B. Artificial Neural Network Evaluation of Concrete Performance Exposed to Elevated Temperature with Destructive-Non-Destructive Tests. *Neural Comput. Appl.* **2024**, *36*, 17079–17093. [CrossRef]
38. Fattah, M.Y.; Al-Haddad, L.A.; Ayasrah, M.M.; Jaber, A.A.; Al-Haddad, S.A. Coupled Finite Element and Artificial Neural Network Analysis of İnterfering Strip Footings in Saturated Cohesive Soils. *Transp. Infrastruct. Geotechnol.* **2024**, *11*, 2168–2185. [CrossRef]
39. Lai, V.Q.; Kounlavong, K.; Chavda, J.T.; Jamsawang, P.; Keawsawasvong, S. Stability Analysis of Buried Pipelines Under Combined Uplift and Lateral Forces Using FELA and ANN. *Appl. Ocean Res.* **2023**, *135*, 103568. [CrossRef]
40. Alnmr, A.; Hosamo, H.H.; Lyu, C.; Ray, R.P.; Alzawi, M.O. Novel Insights in Soil Mechanics: Integrating Experimental Investigation with Machine Learning for Unconfined Compression Parameter Prediction of Expansive Soil. *Appl. Sci.* **2024**, *14*, 4819. [CrossRef]
41. Aslan Topçuoğlu, Y. The Effect of Different Additive Materials on the Engineering Properties of Soils. Ph.D. Thesis, Fırat University, Elazığ, Turkey, 2020.
42. Jamshaid, H.; Mishra, R. A Green Material from Rock: Basalt Fiber-A Review. *J. Text. Inst.* **2015**, *107*, 923–937. [CrossRef]
43. *ASTM D698-12e2*; Standard Test Methods for Laboratory Compaction Characteristics of Soil Using Standard Effort. ASTM International: West Conshohocken, PA, USA, 2012.
44. *ASTM D2166M-16*; Standard Test Method for Unconfined Compressive Strength of Cohesive Soil. ASTM International: West Conshohocken, PA, USA, 2016.
45. Guldemir, H.; Sengur, A. Online Modulation Recognition of Analog Communication Signals Using Neural Network. *Expert Syst. Appl.* **2007**, *33*, 206–214. [CrossRef]
46. Duranay, Z.B. Extreme Learning Machine-Based Power Forecasting in Photovoltaic Systems. *IEEE Access* **2023**, *11*, 128923–128931. [CrossRef]
47. Duranay, Z.B. Neural Network Based Harmonic Elimination in Single-Phase Inverters. *COMPEL-Int. J. Comput. Math. Electr. Electron. Eng.* **2023**, *42*, 543–564. [CrossRef]
48. Aliser, A.; Duranay, Z.B. Fire/Flame Detection with Attention-Based Deep Semantic Segmentation. *Iran J. Sci. Technol. Trans. Electr. Eng.* **2024**, *48*, 705–717. [CrossRef]
49. Guldemir, N.H.; Alkan, A. Classification of Optical Coherence Tomography Images Via Deep Learning. *Firat Univ. J. Eng. Sci.* **2021**, *33*, 607–615.
50. Cao, Z.; Ma, O.; Wang, H. Effect of Basalt Fiber Addition On Static-Dynamic Mechanical Behaviors and Microstructure of Stabilized Soil Compositing Cement And Fly Ash. *Hindawi Adv. Civ. Eng.* **2019**, *2019*, 8214534. [CrossRef]
51. Digioia, A.M.; Huzzo, W.L. Fly Ash Structural Fill. *J. Power Div. ASCE* **1972**, *98*, 77–93. [CrossRef]
52. Koçak, Y. A Study on the Effect of Fly Ash and Silica Fume Substituted Cement Paste and Mortars. *Sci. Res. Essays* **2010**, *5*, 990–998.

Disclaimer/Publisher's Note: The statements, opinions and data contained in all publications are solely those of the individual author(s) and contributor(s) and not of MDPI and/or the editor(s). MDPI and/or the editor(s) disclaim responsibility for any injury to people or property resulting from any ideas, methods, instructions or products referred to in the content.